NANO LETTERS

LETTER

pubs.acs.org/NanoLett

Interface Engineering by Piezoelectric Potential in ZnO-Based Photoelectrochemical Anode

Jian Shi,[†] Matthew B. Starr,[†] Hua Xiang,[†] Yukihiro Hara,[‡] Marc A. Anderson,[‡,∥] Jung-Hun Seo,[§] Zhenqiang Ma,[§] and Xudong Wang*[,†]

[†]Department of Materials Science and Engineering, [‡]Department of Civil and Environmental Engineering, and [§]Department of Electrical and Computer Engineering, University of Wisconsin-Madison, Madison, Wisconsin 53706, United States

[∥]IMDEA Energy Institute, CAT-URJC, Tulipán sn, 28933 Móstoles, Spain

Supporting Information

ABSTRACT: Through a process of photoelectrochemical (PEC) water splitting, we demonstrated an effective strategy for engineering the barrier height of a heterogeneous semiconductor interface by piezoelectric polarization, known as the piezotronic effect. A consistent enhancement or reduction of photocurrent was observed when tensile or compressive strains were applied to the ZnO anode, respectively. The photocurrent variation is attributed to a changed barrier height at the ZnO/ITO interface, which is a result of the remnant piezoelectric potential across the interface due to a nonideal free charge distribution in the ITO electrode. In our system, ~1.5 mV barrier height change per 0.1% applied strain was identified, and 0.21% tensile strain yielded a ~10% improvement of the maximum PEC efficiency. The remnant piezopotential is dictated by the screening length of the materials in contact with piezoelectric component. The difference between this time-independent remnant piezopotential effect and time-dependent piezoelectric effect is also studied in details.

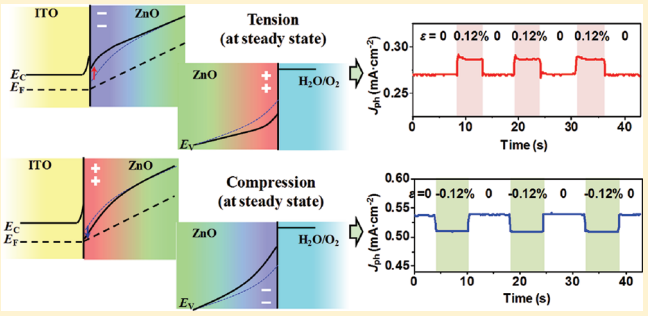

KEYWORDS: ZnO, piezoelectric potential, piezotronics, interface band engineering, photoelectrochemistry

Heterojunctions are a substantial component of electronics, optoelectronics, and electrochemical systems.[1] In most cases, the device functionality is essentially dictated by the interfacial physics and/or chemistry.[2] Interface engineering is thus a critical category for regulating the band alignment, barrier height, and space charge region, and thereby improving the performance or even introducing new functionality to heterojunction-based devices.[2−8] Among the large variety of established/proposed strategies, ionic-displacement induced electric field is a promising and powerful phenomenon for engineering the heterogeneous interface electronic band structure.[3,7−14] Mostly associated with the ferroelectrics' spontaneous polarization, this phenomenon can alter the concentration and type of accumulated/depleted charges at semiconductor/electrolyte interfaces;[6] modulate the barrier height between semiconductors, semiconductor and metal, and metal and ferroelectric insulator;[7−9,13] produce internal electric field in photovoltaic cells;[15] and build band deformation locally.[13] The application of these principles to tunnel junctions,[8] photovoltaics,[15] and photoelectrochemical reactions[10] has demonstrated the practicality and utilization of these effects to enhance device performance.

Nevertheless, most ferroelectric materials are necessarily poor electric conductors, which limit their applications as fundamental building blocks in electronic and optoelectronic devices.[8,9,14,16] Additionally, the existence of multiple polarization domains festooned across the ferroelectric/semiconductor interface complicates the investigation and application of interface band engineering using these materials. In these regards, semiconducting piezoelectric materials could offer a balance between piezoelectric polarization and charge transport properties. ZnO, GaN, and other III-V wurtzite materials are the core semiconductor components in solar cells,[17,18] lasers,[19−22] light emitting diodes (LEDs),[23−25] and photoelectrochemical (PEC) cells.[26−30] These materials also exhibit appreciable piezoelectric effect,[7,11,21,31−33] and thus make good candidates for applying piezoelectric polarization to regulate their semiconductor functionalities. Recently, piezoelectric polarization in ZnO has been found to modulate the band structure of ZnO-related heterojunctions and thus enhanced electron−hole recombination in the application of LED[13] and improved the efficiency of photovoltaic devices.[34,35] The Schottky barrier between ZnO and metal(s) could even be reversed, and thus made ohmic, via piezoelectric polarization, which enabled applications of mechanically switched diodes[33] and memory units.[7,11] The coupling of piezoelectric polarization and the intrinsic electric field in a space charge region for the purpose of tuning charge transport behaviors of

Received: October 23, 2011
Revised: November 15, 2011
Published: November 16, 2011

ACS Publications © 2011 American Chemical Society

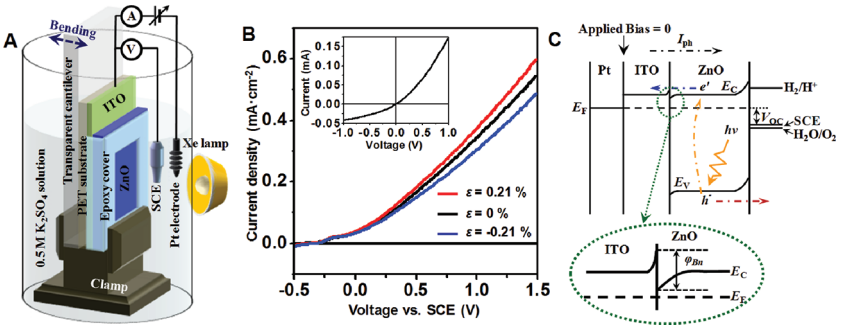

Figure 1. Fundamentals of the PEC cell with piezoelectric ZnO as photoanode. (A) Schematic setup of the ZnO-based PZ-PEC half-cell for characterizing the piezoelectric effect-related water splitting reactions. (B) $J-V$ curves and dark current density of ZnO PEC cell with and without strain applied to the ZnO thin film. Inset is the $I-V$ curve of an as-synthesized ITO-ZnO heterojunction, showing a diode-like performance. (C) Schematic illustration of the band lineup of the entire PEC system. The detailed band alignment of the ITO/ZnO interface is shown in the dashed ellipse. Because of the slightly large work function of ZnO, a Schottky barrier-like n−n junction is formed between ITO and ZnO, where the barrier height is denoted as φ_{Bn}.

semiconductor devices has recently been denoted as the piezotronic effect.[36,37]

In this paper, we report an investigation of barrier-height engineering of a heterogeneous semiconductor interface manifested by a PEC half-cell, where the influence of the remnant piezoelectric polarization on the photocurrent of water splitting was studied as a function of strain applied to the anode. The PEC anode consists of a thin film of piezoelectric ZnO deposited on a transparent ITO electrode. Photocurrent was enhanced when the ZnO anode was subjected to a tensile strain, which was attributed to the barrier height reduction at the indium tin oxide (ITO)−ZnO interface induced by remnant piezoelectric polarization. Effective barrier height change demonstrated a linear relation with mechanical strain. This study suggests a new pathway to engineering the interface barrier without altering the interface structure or chemistry.

The piezoelectric PEC (PZ-PEC) anode was fabricated by sputtering a thin film of ZnO (~1 μm thick) on an ITO/PET substrate. Resistivity of the as-fabricated ZnO film was ~10^7 $\Omega\cdot$cm, which could produce appreciable piezopotential upon deformation as well as reasonable charge conductance for water oxidation under illumination. The device and measurement setup is schematically shown in Figure 1A. The surfaces of ITO, ZnO, and metal wires were sealed by epoxy and only a 2×1 mm^2 working area on ZnO was left open for water oxidation reactions. The flexible PEC film was adhered to the bottom of a PMMA cantilever, which can be deflected to produce various strains. During the measurement, 0.5 M K_2SO_4 aqueous solution was used as electrolyte, saturated calomel electrode (SCE) as reference electrode, and Pt gauze as counter electrode. A potentiostat was employed to control and monitor the PEC process and a Xe lamp served as illumination source.

The $J-V$ characteristic of the ZnO PZ-PEC anode was first measured without applying any strain (black curve in Figure 1B). Photocurrent density (J_{ph}) of 0.54 mA/cm^2 was obtained at applied potential of 1.5 V versus SCE under light intensity of 100 mW/cm^2, demonstrating a considerable water oxidation rate. The dark current remained at a very low level (~5 μA/cm^2) under bias potentials between −0.5 and 1.5 V (vs SCE) indicating the high quality of the ZnO surfaces. Because the nonidealness of interfacial band lineup between ITO transparent electrode and semiconductor electrode is a well-known issue,[2] the ITO/ZnO heterojunction was characterized by measuring the $I-V$ curve directly through the ITO/ZnO layer in air. A slight rectifying effect was observed (inset of Figure 1B) indicating the existence of a small barrier at the ITO/ZnO interface. Based on the reported electron affinities and work functions of ITO and ZnO,[2] the equilibrium band lineups of the complete ZnO PZ-PEC water splitting system is schematically shown in Figure 1C, when no illumination or external bias was applied. In this system, the ITO is supposed to be a highly doped n-type semiconductor and ZnO is an n-type semiconductor as well but with a much lower free charge carrier concentration. The detailed band alignment at the ITO/ZnO interface is shown in the dashed ellipse of Figure 1C. The small barrier, φ_{Bn}, is a likely result of the larger work function of ZnO, corresponding to the $I-V$ characteristic shown in the inset of Figure 1B. It should be noted that due to the much higher carrier concentration of ITO than ZnO, the depletion region in the ITO side is much narrower compared to the accumulation region in ZnO. Under illumination, photogenerated holes in ZnO transport through the ZnO/electrolyte interface and oxidize water. Photogenerated electrons move through the ITO/ZnO interface and eventually reach the counter electrode (Pt) for water reduction. Thus, the heterojunction barrier is an obstacle that restrains the charge transfer and lowers the PEC efficiency.

We herein study the piezoelectric potential produced by straining ZnO and the possible influence on the heterojunction barrier and eventually the PEC performance. The piezoelectric properties of as-prepared ZnO films were first assessed in air under ±0.1% strain and 50 mW/cm^2 illumination from a Xe lamp. The strains were produced by bending the cantilever forward or backward. Because of the significantly larger thickness of the cantilever film (1.3 mm) than the ZnO thin film (~1 μm), the strain experienced by the ZnO film is considered homogeneous compressive or tensile. Potential measurement showed that tensile and compressive strains produced negative and positive polarization at the ITO/ZnO interface, respectively (Supporting Information, Figure S1). The peak piezoelectric potential of ~40 mV was obtained at a strain rate of ~0.1%/s. The relatively small value is a consequence of depolarization induced by photogenerated free electrons and holes in ZnO.

The $J-V$ curves were then collected when the ZnO anode was under strain. As shown in Figure 1B, an enhanced photocurrent (I_{ph}) was observed when a 0.21% tensile strain was applied. At applied potential of 1.5 V versus SCE and under light intensity of

dx.doi.org/10.1021/nl203729j |Nano Lett. 2011, 11, 5587–5593

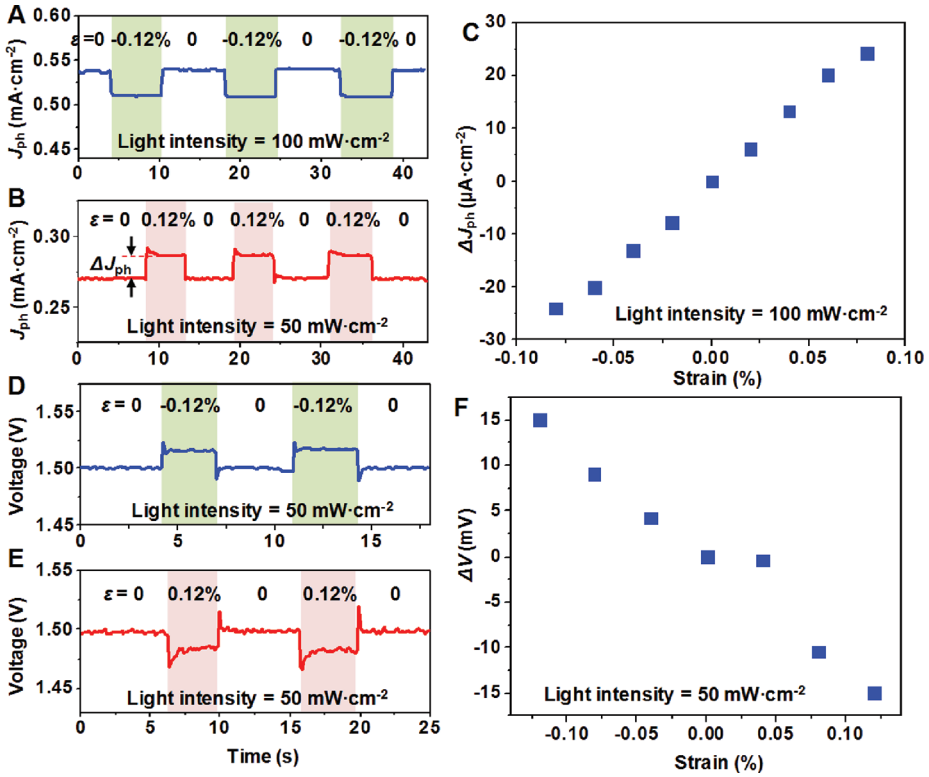

Figure 2. PEC performance when ZnO was under static strains. (A) Photocurrent density (J_{ph}) of the ZnO PZ-PEC under periodic compressive strains (−0.12%) at an applied bias of 1.5 V versus SCE. The strained regions are marked with a shade of light green. J_{ph} was collected under illumination of 100 mW/cm^2. (B) J_{ph} under periodic tensile strains when light intensity was 50 mW/cm^2 and applied bias was 1.5 V versus SCE. Current spikes can be observed at the moments of applying and releasing strain due to the lower light intensity. (C) Photocurrent density change (ΔJ_{ph}) as a function of applied strain under illumination of 100 mW/cm^2. The background J_{ph} was 540 μA/cm^2 and applied bias was 1.5 V versus SCE. (D,E) Applied bias (V) under periodic compressive (−0.12%) (D) and tensile (0.12%) (E) strains measured by galvanostat. The light intensity was kept at 50 mW/cm^2. (F) Applied bias change (ΔV) as a function of applied strain under illumination of 50 mW/cm^2.

100 mW/cm^2, J_{ph} increased from ∼0.54 to ∼0.6 mA/cm^2 due to the tensile strain. The maximum efficiency was calculated from the $J-V$ curves and a ∼10.2% efficiency increase was identified (from 0.06 to 0.066% Figure S2 in Supporting Information). Opposite effect was observed under 0.21% compressive strain, which induced reduced J_{ph} (blue curve in Figure 1B) and a ∼8.5% maximum efficiency drop (from 0.06 to 0.055%).

It is known that the piezoelectric potential and associated current outputs are always in the form of pulses because of the quick balance of the polarization through external charge flow. However, in our PZ-PEC system, the strain induced I_{ph} change was found constant. In order to fully understand this phenomenon, I_{ph} was measured at fixed voltage as a function of strain. Figure 2A,B presents the J_{ph} measured by the potentiostat when a constant strain was applied to the ZnO anode periodically, where the applied external bias was fixed as 1.5 V versus SCE. With a compressive strain of −0.12%, J_{ph} decreased from 542 to 509 μA/cm^2 when the illumination intensity was 100 mW/cm^2. While with a tensile strain of 0.12%, J_{ph} increased from 269 to 287 μA/cm^2 under a light intensity of 50 mW/cm^2. Small spikes could be observed from the J_{ph} profiles at the moment of applying and releasing strain when the light intensity was 50 mW/cm^2 (Figure 2B). Response of J_{ph} on straining is swift and highly reproducible. More importantly, the J_{ph} change (ΔJ_{ph}) is independent of time. No decay was observed during a period extending over hundreds of seconds, as long as the strain was held (not including the initial spikes, see Supporting Information Figure S3). Thus, ΔJ_{ph} is defined as the difference between the constant J_{ph} under strain and the J_{ph} baseline when no strain was applied. The relationship between ΔJ_{ph} and strain is found to be approximately linear as shown in Figure 2C, where all data were collected under light intensity of 100 mW/cm^2.

In order to confirm that the ΔJ_{ph} is associated with the piezoelectric effect in strained ZnO, a series of control experiments was conducted by replacing ZnO with TiO_2, because it does not possess piezoelectric property but does have a similar band structure as ZnO.[26,38] TiO_2 thin films were deposited on the same ITO/PET substrates by atomic layer deposition (ALD) and tested under the identical experimental conditions. Applying and releasing strain did not yield any current change to the J_{ph} of TiO_2 PEC anode (Supporting Information Figure S4), which ruled out any current change that was the result of the anode shape or position change during bending and confirmed the role of piezoelectric effect of ZnO on altering the PEC photocurrent.

Galvanostat measurements were conducted to demonstrate that the piezoelectric effect can also adjust the applied bias accordingly to achieve the same PEC J_{ph} (Figure 2D,E). Experiments were conducted under a light intensity of 50 mW/cm^2. As shown in Figure 2D, a compressive strain of −0.12% shifted the applied bias from 1.50 V versus SCE to 1.515 V versus SCE, suggesting that a higher bias potential was required to keep current unchanged during compressive strain. When the PEC anode was under tensile strain, a lower bias (from 1.50 V versus SCE to 1.485 V versus SCE) was found sufficient to pull equal J_{ph}

dx.doi.org/10.1021/nl203729j |Nano Lett. 2011, 11, 5587–5593

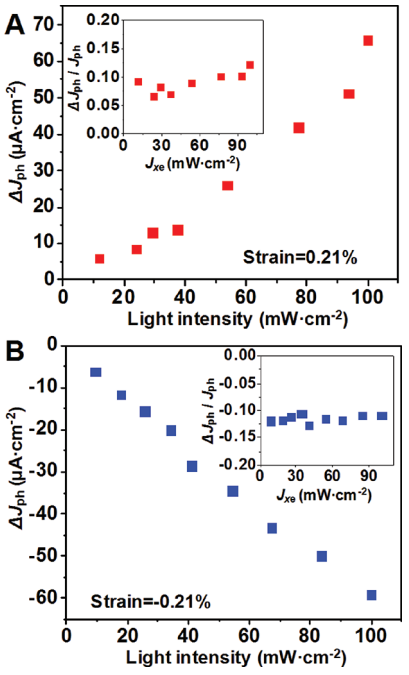

Figure 3. Light intensity influence to photocurrent density change (ΔJ_{ph}). ΔJ_{ph} as a function of light intensity from 10 to 100 mW/cm^2 under a static tensile (0.12%) (A) and compressive (−0.12%) (B) strain. Insets of (A) and (B) are the relative photocurrent density change (the ratio between ΔJ_{ph} and J_{ph} at constant strain) under different light intensities. A nearly constant $\Delta J_{ph}/J_{ph}$ value can be observed.

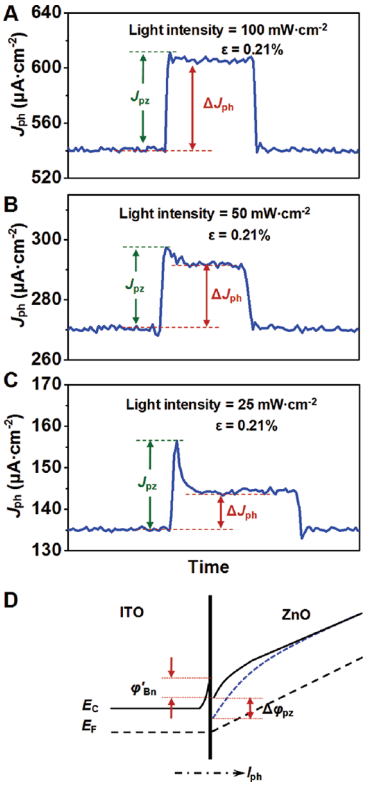

Figure 4. J_{ph} characteristics under different light intensities and corresponding band structure. (A−C) J_{ph} variation profiles recorded under light intensity of 100, 50, and 25 mW·cm^{-2}, respectively, when the ZnO PEC anode was subjected to a constant 0.21 tensile strain. J_{ph} spikes correspond to the piezopotential-driven charge flow through the external circuit when the piezoelectric polarization is not completely compensated by internal photogenerated charges. They are denoted as J_{pz}. The following constant J_{ph} increase was due to interface barrier height change and is denoted as ΔJ_{ph}. Lower light intensity resulted in larger J_{pz} but smaller ΔJ_{ph}, thus more significant initial J_{ph} spikes were recorded. (D) Schematic band structure change at the ITO/ZnO interface under a constant tensile strain.

(Figure 2E). Similar to ΔJ_{ph}, change of the applied bias (ΔV) exhibited a linear relationship to the strain under the same light illumination (50 mW/cm^2), as shown in Figure 2F.

The influence of light intensity to ΔJ_{ph} was further investigated. Light intensities ranging from 10 to 100 mW/cm^2 were applied when the strain of the PZ-PEC was kept constant. Figure 3A clearly shows that ΔJ_{ph} increased monotonically with the increasing light intensity, when the PZ-PEC anode was under a constant tensile strain of 0.21%. A J_{ph} increase of as high as 67 μA/cm^2 was recorded under 100 mW/cm^2 light intensity. Because J_{ph} also increases linearly with the light intensity, the relative photocurrent enhancement ($\Delta J_{ph}/J_{ph}$) was calculated and plotted in the inset of Figure 3A. Such a ratio appeared to be independent to the light intensity and remained around the value of ∼8%. Similar relationship was obtained from compressive strains (Figure 3B). The ratio of $\Delta J_{ph}/J_{ph}$ remained at ∼−12% under a compressive strain of −0.21% regardless of the light intensity (inset of Figure 3B). The near constant value of $\Delta J_{ph}/J_{ph}$ in both cases (compressive and tensile straining) implies that the photogenerated free charge carriers have no influence on the ratio of photocurrent change, although they do modify the conductivity of the ZnO film as well as the magnitude of piezoelectric potential pulses (Supporting Information Figure S5C). The larger absolute value of $\Delta J_{ph}/J_{ph}$ from compressive strain is possibly due to the dissociation of domains in the polycrystalline ZnO film during tensile straining which degrades the piezoelectric property.

The observed characteristic J_{ph} changes can be understood from the band structure when the ZnO PZ-PEC anode is under strain (see Supporting Information Figure S6 for schematic band structures).[39] Experimental measurements showed that when a tensile strain was applied to the ZnO film, the surface in contact with ITO appeared negative and the other side appeared positive (Supporting Information Figure S2). The piezoelectric potential induces a linear tilt of the bands and Fermi level along the thickness direction of the ZnO film. This band bending causes immediate free charge redistribution inside the ZnO film and results in a recovery of band flatness. Thus, the measured piezoelectric potential (V_{pz}) represents the amplitude of the surface Fermi level shifting after internal free charge screening. The V_{pz} will quickly drop to zero due to charge transport through the external circuit driven by the piezopotential. Therefore the measured V_{pz}'s are always in the form of pulses. V_{pz} is directly proportional to the amplitude of strain (Supporting Information Figure S5A) and decreases with the increasing of incident light intensity (Supporting Information Figure S5B,C). When the ZnO anode was under illumination and an external bias, J_{ph} flowed from ITO through ZnO to the electrolyte. The strain-induced V_{pz} created an instantaneous piezocurrent (J_{pz}) with the same direction as J_{ph}. Therefore, a quick increasing of current density ($J_{ph} + J_{pz}$) was observed (as marked in Figure 4A−C). J_{pz} drops together with V_{pz}, resulting in a positive current pulse when a tensile strain is applied. When V_{pz} dropped back to zero

dx.doi.org/10.1021/nl203729j |Nano Lett. 2011, 11, 5587–5593

due to J_{pz}, the piezo-PEC system reached a steady state, although the anode was still under tension.

At the steady state, the piezopotential is completely screened outside of the ITO space charge region and no more piezo-current can be induced ($J_{pz} = 0$). However, due to the nonideal interface of ITO/ZnO and ZnO/electrolyte (i.e., finite screening length), there always exists a remnant polarization at both interfaces. This situation is equivalent to the well-known remnant internal electric field of ferroelectric materials in a short-circuit condition.[8,40] The remnant negative piezoelectric charges at the ITO/ZnO interface moves up the conduction band of ZnO locally, as shown in Figure 4B, where the amplitude of the interface band shift is denoted as $\Delta\varphi_{pz}$. Similar effect can also be induced in ITO. But due to the very narrow depletion layer of ITO, band shifting on the ITO side is ignored here. Thus, the barrier height between ITO and ZnO is reduced to $\varphi'_{Bn} = \varphi_{Bn} - \Delta\varphi_{pz}$, which results in an increase of thermionic current through the interface. Likewise, bending of the valence band of ZnO at the electrolyte side could also be reduced due to the remnant positive piezoelectric charges. However, due to the ohmic-like contact between ZnO and electrolyte, a slight change on the interface band bending would contribute trivial in suppressing or augmenting effective charge transportation, especially when the original driving force on hole transfer is huge. Consequently, a constant photocurrent increase (ΔJ_{ph}) is observed when a tensile strain is maintained in the piezo-PEC anode.

It is important to note that ΔJ_{ph} is induced by the piezoelectric polarization but via a different mechanism from that of the J_{pz} pulses. ΔJ_{ph} is determined by the interfacial barrier height change due to the remnant polarization, which is a result of the local charge distribution at the interface after the piezopotential-induced charge redistribution reaches equilibrium. This phenomenon is related to the strain and interfacial material property but is independent of the concentration of free charge carriers inside ZnO. Therefore, the relative current change (or $\Delta J_{ph}/J_{ph}$ as shown in Figure 3) remains a constant under various incident light intensities. However, J_{pz} is directly related to the apparent piezoelectric potential V_{pz}, and thus the incident light intensity dictates the amplitude of J_{pz}. Under low light intensity, the piezocurrent is more prominent than the constant photocurrent change ($\Delta J_{ph} < J_{pz}$), thus an initial current spike was observed corresponding to J_{pz} (Figure 4A,B). Under high light intensity, the piezocurrent immerges into the constant photocurrent change ($\Delta J_{ph} > J_{pz}$), thus a square current curve was obtained (Figure 4C).

The same mechanism applies to the case of compressive strain where J_{pz} had opposite direction as J_{ph}. Thus negative current peaks were produced. When steady state was reached under a constant compressive strain, the remnant piezopotential at ITO/ZnO interface was positive and thus enlarged the ITO/ZnO barrier height, reducing J_{ph}.

We have shown that the remnant polarization of a piezoelectric semiconductor material is important in regulating its electronic performance. For a Schokky barrier-like heterojunction, the $J-V$ characteristic is governed by equation[1]

$$J = C_0 T^2 \exp\left[\frac{-q(\varphi_{Bn} + \Delta\varphi_{pz})}{kT}\right]\left[\exp\left(\frac{qV}{nkT}\right) - 1\right] \quad (1)$$

where C_0 is a constant, q is the elementary charge, k is the Boltzmann constant, T is temperature, n is ideality factor, V is the applied potential, φ_{Bn} is the original barrier height, and $\Delta\varphi_{pz}$ if the effective barrier height change by remnant polarization. This equation shows that even if the remnant polarization-induced barrier height change is small, the variation in current can still be significant. Using the $\Delta J_{ph}/J_{ph}$ data obtained from PZ-PEC measurements, $\Delta\varphi_{pz}$ was calculated as a function of strain and plotted in Figure 5A. The relation between $\Delta\varphi_{pz}$ and strain appeared to be linear, with a barrier height decrease of ~1.5 mV per 0.1% strain applied.

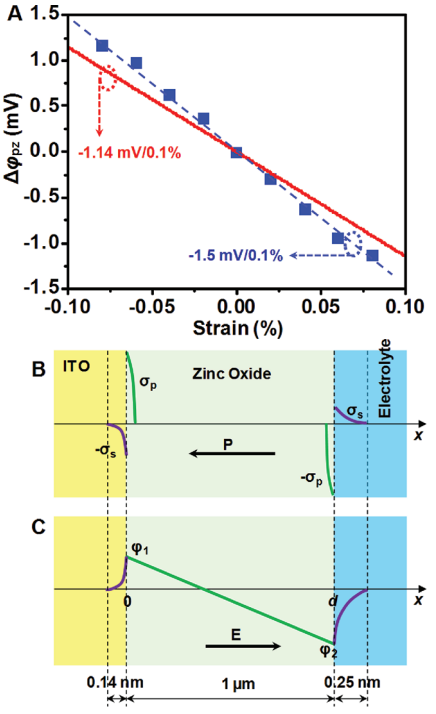

Figure 5. Barrier height change ($\Delta\varphi_{pz}$) as a function of strain. (A) $\Delta\varphi_{pz}$ determined from experimental results (blue squares) gives a barrier height change of −1.5 mV per 0.1% applied strain. Calculated relationship (red line) shows a smaller changing rate (−1.14 mV per 0.1% applied strain) possibly due to the deviation of screen lengths estimation. (B,C) Schematic diagrams of the charge density distributions (B) and potential profiles (C) in ZnO, ITO, and electrolyte solution.

Approaches for calculating the depolarization field in ferroelectric materials were employed here to quantitatively understand the relationship between strain and $\Delta\varphi_{pz}$.[8,40] In our model, ZnO was regarded as a piezoelectric film sandwiched between two electrodes, ITO and electrolyte (Figure 5B). At steady state, the piezoelectric polarization P in ZnO film creates surface charge densities $\pm\sigma_P$, which induce screening charge densities $\mp\sigma_S$ on the two electrodes following equation:

$$\sigma_S = \frac{d}{\varepsilon_r(\delta_1 + \delta_2) + d}P \quad (2)$$

where δ_1 and δ_2 are the charge screening length of ITO and electrolyte, respectively, d is the thickness of ZnO film, and ε_r is the relative permittivity of ZnO (8.5). On the basis of Thomas-Fermi screening length approximation, δ_1 and δ_2 were calculated to be 0.14 and 0.25 nm, respectively.[41,42] The remnant polarization is due to $\sigma_P > \sigma_S$ in a nonideal electrode material ($\delta \neq 0$), which induces a linear electric potential distribution in ZnO $\varphi(x) = \varphi_1 - (x/(\varepsilon_r\varepsilon_0)(P - \sigma_S)$, and an exponential potential decay in the screening regions of the two electrodes, as shown in Figure 5C. The interface barrier height change $\Delta\varphi_{pz}$ is equivalent to the remnant potential at the ITO/ZnO interface φ_1. For simplicity, the ITO/ZnO/electrolyte is assumed to be short-circuited

dx.doi.org/10.1021/nl203729j |Nano Lett. 2011, 11, 5587–5593

and $\Delta\varphi_{pz}$ is therefore given by

$$\Delta\varphi_{pz} = \varphi_1 = \frac{\delta_1 d}{\varepsilon_0[\varepsilon_r(\delta_1 + \delta_2) + d]} d_{31} E\varepsilon \quad (3)$$

where d_{31}, E, and ε are the piezoelectric coefficient, Young's modulus and strain of the ZnO anode. Calculation revealed a linear relationship between $\Delta\varphi_{pz}$ and strain with a slope (−1.14 mV/0.1%) slightly smaller than the experimental result (−1.5 mV/0.1%) (Figure 5A), which is likely due to deviation of the screen length estimation. This analysis further demonstrated that the remnant polarization and barrier height change is dependent on the materials used and their interface properties. The small absolute value of barrier height change and the corresponding small efficiency improvement is due to the metal-like behavior of ITO, which leaves a very small space of improvement. A more pronounced barrier height change would be possible at the interface of ZnO and other semiconductor materials that have longer screening length than ITO.

In summary, we have demonstrated a strain-related photocurrent variation using a ZnO-based PZ-PEC anode. The photocurrent increased/decreased by a fixed amount when the PZ-PEC anode was under a constant tensile/compressive strain, respectively. The relative photocurrent change is found linearly related to the applied strain but independent to the incident light intensity. The constant photocurrent change is explained by the remnant polarization at the ZnO/ITO interface under strain, which resulted in a slight variation of barrier height. This phenomenon is different from the piezopotential-drvien current flow, although it is also resulted from the piezoelectric effect. From our ZnO/ITO anode system, the barrier height change was found to be small (~1.5 mV at 0.1% strain), but the resulted photocurrent change could be significant (5.6%) due to the exponential dependence of current on barrier height. The remnant polarization is dependent upon both material and interface properties and a larger barrier height change can be expected for other semiconductor-piezoelectric material interfaces. Our system showed a ~10% maximum efficiency increase under 0.21% tensile strain and the improvement could be much larger for systems that hold higher remnant piezopotential. This discovery could render a new pathway for engineering the interface barrier, which is promising for improving the efficiency of many electronics, optoelectronics, and photovoltaic devices.

■ ASSOCIATED CONTENT

Supporting Information. Additional information and figures, including experimental details, piezoelectric responses of ZnO films, PEC efficiency calculation, long-time current response under strain, control experiments, and schematic band lineup of ITO-ZnO-Electrolyte subject to piezopotential and under external bias. This material is available free of charge via the Internet at http://pubs.acs.org.

■ AUTHOR INFORMATION

Corresponding Author
*E-mail: xudong@engr.wisc.edu.

■ ACKNOWLEDGMENT

J.S., M.B.S., and X.W. thank the support of National Science Foundation under Grant DMR-0905914, DARPA under Grant N66001-11-1-4139, and the UW-Madison graduate school. J.H.S. and Z.M. are supported by PECASE award, FA9550-091-0482. The program manager is Dr. Gernot Pomrenke.

■ REFERENCES

(1) Sze, S. M.; Ng, K. K. *Physics of Semiconductor Devices*, 3rd ed.; Wiley-Interscience: New York, 2007.
(2) Wager, J. F. Transparent electronics: Schottky barrier and heterojunction considerations. *Thin Solid Films* **2008**, *516*, 1755–1764.
(3) Dunn, S.; Tiwari, D. Photochemistry on a polarisable semiconductor: what do we understand today? *J. Mater. Sci.* **2009**, *44*, 5063–5079.
(4) McKone, J. R.; Warren, E. L.; Bierman, M. J.; Boettcher, S. W.; Brunschwig, B. S.; Lewis, N. S.; Gray, H. B. Evaluation of Pt, Ni, and Ni-Mo electrocatalysts for hydrogen evolution on crystalline Si electrodes. *Energy Environ. Sci.* **2011**, *4*, 3573–3583.
(5) Perego, M.; Seguini, G.; Scarel, G.; Fanciulli, M.; Wallrapp, F. Energy band alignment at $TiO_{(2)}$/Si interface with various interlayers. *J. Appl. Phys.* **2008**, *103*, 043509–043514.
(6) Rohrer, G. S.; Giocondi, J. L.; Salvador, P. A. The origin of photochemical anisotropy in $SrTiO_3$. *Top. Catal.* **2007**, *44*, 529–533.
(7) Song, J. H.; Zhang, Y.; Xu, C.; Wu, W. Z.; Wang, Z. L. Polar Charges Induced Electric Hysteresis of ZnO Nano/Microwire for Fast Data Storage. *Nano Lett.* **2011**, *11*, 2829–2834.
(8) Zhuravlev, M. Y.; Sabirianov, R. F.; Jaswal, S. S.; Tsymbal, E. Y. Giant electroresistance in ferroelectric tunnel junctions. *Phys. Rev. Lett.* **2005**, *94*, 246802–246805.
(9) Cheong, S. W.; Choi, T.; Lee, S.; Choi, Y. J.; Kiryukhin, V. Switchable Ferroelectric Diode and Photovoltaic Effect in $BiFeO_{(3)}$. *Science* **2009**, *324*, 63–66.
(10) Rohrer, G. S.; Burbure, N. V.; Salvador, P. A. Photochemical Reactivity of Titania Films on $BaTiO_{(3)}$ Substrates: Origin of Spatial Selectivity. *Chem. Mater.* **2010**, *22*, 5823–5830.
(11) Wu, W. Z.; Wang, Z. L. Piezotronic Nanowire-Based Resistive Switches As Programmable Electromechanical Memories. *Nano Lett.* **2011**, *11*, 2779–2785.
(12) Zhang, Y.; Liu, Y.; Wang, Z. L. Fundamental Theory of Piezotronics. *Adv. Mater.* **2011**, *23*, 3004–3013.
(13) Yang, Q.; Wang, W.; Xu, S.; Wang, Z. L. Enhancing Light Emission of ZnO Microwire-Based Diodes by Piezo-Phototronic Effect. *Nano Lett.* **2011**, *11*, 4012–4017.
(14) Yang, S. Y.; Seidel, J.; Byrnes, S. J.; Shafer, P.; Yang, C. H.; Rossell, M. D.; Yu, P.; Chu, Y. H.; Scott, J. F.; Ager, J. W.; Martin, L. W.; Ramesh, R. Above-bandgap voltages from ferroelectric photovoltaic devices. *Nat. Nanotechnol.* **2010**, *5*, 143–147.
(15) Huang, J. S.; Yuan, Y. B.; Reece, T. J.; Sharma, P.; Poddar, S.; Ducharme, S.; Gruverman, A.; Yang, Y. Efficiency enhancement in organic solar cells with ferroelectric polymers. *Nat. Mater.* **2011**, *10*, 296–302.
(16) Huang, H. T. Solar Energy Ferroelectric photovoltaics. *Nat. Photonics* **2010**, *4*, 134–135.
(17) Law, M.; Greene, L. E.; Johnson, J. C.; Saykally, R.; Yang, P. D. Nanowire dye-sensitized solar cells. *Nat. Mater.* **2005**, *4*, 455–459.
(18) Lee, C. S.; Tang, Y. B.; Chen, Z. H.; Song, H. S.; Cong, H. T.; Cheng, H. M.; Zhang, W. J.; Bello, I.; Lee, S. T. Vertically Aligned p-Type Single-Crystalline GaN Nanorod Arrays on n-Type Si for Heterojunction Photovoltaic Cells. *Nano Lett.* **2008**, *8*, 4191–4195.
(19) Bagnall, D. M.; Chen, Y. F.; Zhu, Z.; Yao, T.; Koyama, S.; Shen, M. Y.; Goto, T. Optically pumped lasing of ZnO at room temperature. *Appl. Phys. Lett.* **1997**, *70*, 2230–2232.
(20) Chu, S.; Wang, G. P.; Zhou, W. H.; Lin, Y. Q.; Chernyak, L.; Zhao, J. Z.; Kong, J. Y.; Li, L.; Ren, J. J.; Liu, J. L. Electrically pumped waveguide lasing from ZnO nanowires. *Nat. Nanotechnol.* **2011**, *6*, 506–510.
(21) Park, S. H.; Chuang, S. L. Piezoelectric effects on electrical and optical properties of wurtzite GaN/AlGaN quantum well lasers. *Appl. Phys. Lett.* **1998**, *72*, 3103–3105.

(22) Vispute, R. D.; Talyansky, V.; Choopun, S.; Sharma, R. P.; Venkatesan, T.; He, M.; Tang, X.; Halpern, J. B.; Spencer, M. G.; Li, Y. X.; Salamanca-Riba, L. G.; Iliadis, A. A.; Jones, K. A. Heteroepitaxy of ZnO on GaN and its implications for fabrication of hybrid optoelectronic devices. *Appl. Phys. Lett.* **1998**, *73*, 348–350.

(23) Alivov, Y. I.; Kalinina, E. V.; Cherenkov, A. E.; Look, D. C.; Ataev, B. M.; Omaev, A. K.; Chukichev, M. V.; Bagnall, D. M. Fabrication and characterization of n-ZnO/p-AlGaN heterojunction light-emitting diodes on 6H-SiC substrates. *Appl. Phys. Lett.* **2003**, *83*, 4719–4721.

(24) Alivov, Y. I.; Van Nostrand, J. E.; Look, D. C.; Chukichev, M. V.; Ataev, B. M. Observation of 430 nm electroluminescence from ZnO/GaN heterojunction light-emitting diodes. *Appl. Phys. Lett.* **2003**, *83*, 2943–2945.

(25) Park, S. J.; Hwang, D. K.; Kang, S. H.; Lim, J. H.; Yang, E. J.; Oh, J. Y.; Yang, J. H. p-ZnO/n-GaN heterostructure ZnO light-emitting diodes. *Appl. Phys. Lett.* **2005**, *86*, 222101–222103.

(26) Chen, X. B.; Shen, S. H.; Guo, L. J.; Mao, S. S. Semiconductor-based Photocatalytic Hydrogen Generation. *Chem. Rev.* **2010**, *110*, 6503–6570.

(27) Fujii, K.; Ohkawa, K. Photoelectrochemical properties of p-type GaN in comparison with n-type GaN. *Jpn. J. Appl. Phys., Part 2* **2005**, *44*, L909–L911.

(28) Ono, M.; Fujii, K.; Ito, T.; Iwaki, Y.; Hirako, A.; Yao, T.; Ohkawa, K. Photoelectrochemical reaction and H-2 generation at zero bias optimized by carrier concentration of n-type GaN. *J. Chem. Phys.* **2007**, *126*, 054708–054714.

(29) Wolcott, A.; Smith, W. A.; Kuykendall, T. R.; Zhao, Y. P.; Zhang, J. Z. Photoelectrochemical Study of Nanostructured ZnO Thin Films for Hydrogen Generation from Water Splitting. *Adv. Funct. Mater.* **2009**, *19*, 1849–1856.

(30) Zhang, J. Z.; Yang, X. Y.; Wolcott, A.; Wang, G. M.; Sobo, A.; Fitzmorris, R. C.; Qian, F.; Li, Y. Nitrogen-Doped ZnO Nanowire Arrays for Photoelectrochemical Water Splitting. *Nano Lett.* **2009**, *9*, 2331–2336.

(31) Bernardini, F.; Fiorentini, V.; Vanderbilt, D. Spontaneous polarization and piezoelectric constants of III-V nitrides. *Phys. Rev. B* **1997**, *56*, 10024–10027.

(32) Bykhovski, A.; Gelmont, B.; Shur, M.; Khan, A. Current-Voltage Characteristics of Strained Piezoelectric Structures. *J. Appl. Phys.* **1995**, *77*, 1616–1620.

(33) Zhou, J.; Fei, P.; Gu, Y. D.; Mai, W. J.; Gao, Y. F.; Yang, R.; Bao, G.; Wang, Z. L. Piezoelectric-Potential-Controlled Polarity-Reversible Schottky Diodes and Switches of ZnO Wires. *Nano Lett.* **2008**, *8*, 3973–3977.

(34) Yang, Y.; Guo, W.; Zhang, Y.; Ding, Y.; Wang, X.; Wang, Z. L. Piezotronic Effect on the Output Voltage of P3HT/ZnO Micro/Nanowire Heterojunction Solar Cells. *Nano Lett.* **2011**, *11*, 4812–4817.

(35) Hu, Y.; Zhang, Y.; Chang, Y.; Snyder, R. L.; Wang, Z. L. Optimizing the Power Output of a ZnO Photocell by Piezopotential. *ACS Nano* **2010**, *4*, 4220–4224.

(36) Wang, Z. L. Piezopotential gated nanowire devices: Piezotronics and piezo-phototronics. *Nano Today* **2010**, *5*, 540–552.

(37) Wang, Z. L. Piezotronic and Piezophototronic Effects. *J. Phys. Chem. Lett.* **2010**, *1*, 1388–1393.

(38) Thimsen, E.; Paracchino, A.; Laporte, V.; Sivula, K.; Gratzel, M. Highly active oxide photocathode for photoelectrochemical water reduction. *Nat. Mater.* **2011**, *10*, 456–461.

(39) Pan, C.; Li, Z.; Guo, W.; Zhu, J.; Wang, Z. L. Fiber-Based Hybrid Nanogenerators for/as Self-Powered Systems in Biological Liquid. *Angew. Chem., Int. Ed.* **2011**, *50*, 11192–11196.

(40) Mehta, R. R.; Silverma., Bd; Jacobs, J. T. Depolarization Fields in Thin Ferroelectric Films. *J. Appl. Phys.* **1973**, *44*, 3379–3385.

(41) Cheung, C. K.; Wang, R. X.; Beling, C. D.; Djurisic, A. B.; Fung, S. Positron beam study of indium tin oxide films on GaN. *J. Phys.: Condens. Matter* **2007**, *19*, 086204–086213.

(42) Israelachvili, J. N. *Intermolecular and Surface Forces*, 3rd ed.; Academic Press: Boston, 2010; p 710.